



INTERNATIONAL ATOMIC ENERGY AGENCY

FIFTEENTH INTERNATIONAL CONFERENCE ON PLASMA PHYSICS
AND CONTROLLED NUCLEAR FUSION RESEARCH

Seville, Spain, 26 September – 1 October 1994

IAEA-CN-60/ E-P-3

Conf-940933--10

**Projection of ITER Performance Using the Multi-Machine L- and H-
Mode Databases**

ITER Confinement Database and Modeling Group*

presented by S.M. Kaye, Princeton Plasma Physics Laboratory,
Princeton N.J. 08543 U.S.A.

* Alcator C-Mod:	J.A. Snipes, R.S. Granetz, M. Greenwald
ASDEX:	F. Ryter, O.J.W.F. Kardaun, U. Stroth, A. Kus
ASDEX-Upgrade:	F. Ryter
Compass-D:	P.G. Carolan, S.J. Fielding, M. Valovic
DIII & DIII-D:	J.C. DeBoo, T. Carlstrom, D.P. Schissel
FT-U:	G. Bracco
JET:	K. Thomsen, D.J. Campbell, J.P. Christiansen, J.G. Cordey
JFT-2M:	Y. Miura, N. Suzuki, M. Mori, T. Matsuda, H. Tamai, T. Takizuka, S.-I. Itoh, K. Itoh
JT-60:	M. Kikuchi, O. Naito
PBX-M & PDX:	S.M. Kaye
TEXTOR:	J. Ongena
TORE-SUPRA:	G.T. Hoang

MASTER

This is a preprint of a paper intended for presentation at a scientific meeting. Because of the provisional nature of its content and since changes of substance or detail may have to be made before publication, the preprint is made available on the understanding that it will not be cited in the literature or in any way be reproduced in its present form. The views expressed and the statements made remain the responsibility of the named author(s); the views do not necessarily reflect those of the government of the designating Member State(s) or of the designating organization(s). In particular, neither the IAEA nor any other organization or body sponsoring this meeting can be held responsible for any material reproduced in this preprint.

Se

DISCLAIMER

This report was prepared as an account of work sponsored by an agency of the United States Government. Neither the United States Government nor any agency thereof, nor any of their employees, makes any warranty, express or implied, or assumes any legal liability or responsibility for the accuracy, completeness, or usefulness of any information, apparatus, product, or process disclosed, or represents that its use would not infringe privately owned rights. Reference herein to any specific commercial product, process, or service by trade name, trademark, manufacturer, or otherwise does not necessarily constitute or imply its endorsement, recommendation, or favoring by the United States Government or any agency thereof. The views and opinions of authors expressed herein do not necessarily state or reflect those of the United States Government or any agency thereof.

DISCLAIMER

Portions of this document may be illegible in electronic image products. Images are produced from the best available original document.

Projection of ITER Performance Using the Multi-Machine L- and H-Mode Databases

Abstract

An overview of recent analyses of H- and L-mode confinement and L- to H-mode threshold data is presented. The standard subset of the H-mode database, consisting of about 1600 time slices from six tokamaks, leads to power law scalings for ELMy and ELM-free discharges, both of which predict a confinement time for ITER of approximately 5.5 sec. The analysis indicates a strong dependence of confinement time scaling and prediction on the neutral penetration from the divertor into the main chamber. Consideration of dimensionless variables suggest scaling expressions for the H-mode threshold which predict threshold powers for ITER of between 100 and 200 MW. Finally, the L-mode database has been updated to contain over 1500 time-slices from eleven tokamaks. A preliminary empirical scaling based on the total confinement time has been developed.

1. Introduction

The H-mode database working group effort was initiated in 1989 in order to compile the data necessary to determine the confinement expectations of ITER and other future devices. The group has compiled H-mode confinement data from six devices, and has determined both global and thermal confinement scalings under various assumptions constraining the data. The group has also compiled L- to H-mode threshold data in order to determine quantitatively the required power for transition into the H-mode as a function of controllable discharge parameters. The L-mode database has recently been updated, adding new data from various devices as well as adding additional parameters for discharges that were already in the database. The group is also compiling profile data to provide a set of discharges on which transport model development and testing can be based.

This paper will serve as an update on the first three areas of activity, as the compilation of the profile database has just started.

2. H-mode Confinement

The first version of the H-mode confinement database, ITERHDB.1 (DB1), was released for public use at the end of 1990 [1]. In 1991, the existing data in DB1 were improved, and new H-mode data were added. The major data additions to the database, ITERHDB.2 (DB2), come from experiments with different wall conditioning techniques, parameter scans, operational scenarios, and with auxiliary heating by means other than pure neutral beam injection. Furthermore, improvements to the old data include better estimates of the fast ion energy content for all machines and diamagnetic energy estimates for PDX. A detailed description of these improvements can be found in [2].

As was done for DB1, a set of criteria defining a "standard" dataset was developed. The criteria, detailed in [2], are similar to those developed for DB1, constraining on time stationary behavior, low fast hot ion content and radiation losses, no pellet injection, H° or D° NBI injection only, no low-q or β-limit discharges, no hot ion H-modes, and no JET data from 1987. A total of 1627 out of a total of 3405 H-mode time-slices satisfied these constraints (769 ELMy and 858 ELM-free).

Simple power law regression estimates of both the global and thermal energy confinement time for ELMy (all ELM types) and ELM-free data in the standard dataset

were performed for EPS '93 [3]. The differences in scaling results between [3] and earlier work [1] stemmed primarily from having better estimates of fast ion energy content, treatment of open vs. closed divertor data (see below), and the omission of 1987 JET data. The regression results from [3] for the thermal energy confinement are:

$$\tau_{th}^{ELMy} = 0.022 I_P^{0.76} B_T^{0.15} P_{Lth}^{-0.70} M^{0.30} R^{2.60} n_e^{0.42} \epsilon^{0.30} \kappa^{1.05} \quad (1)$$

and

$$\tau_{th}^{ELM-free} = 0.036 I_P^{1.06} B_T^{0.32} P_{Lth}^{-0.67} M^{0.41} R^{1.79} n_e^{0.17} \epsilon^{-0.11} \kappa^{0.66} \quad (2)$$

in units of sec., MA, T, MW, AMU, m, and 10^{19} m^{-3} . P_{Lth} is total heating power corrected for shine-thru, bad orbit, and charge-exchange losses, less the time rate of change of the stored energy. The two scalings have an rms error of 13.8% and 12.3% respectively, and plots of the experimental thermal energy confinement time vs. the scaling value are shown in Figs. 1a and 1b. Using EDA baseline parameters for ITER (24 MA, 5.7 T, 310 MW auxiliary heating power, $M=2.5$, $R=8.1$ m, $n_e = \langle n_e \rangle = 1.1 \times 10^{20} \text{ m}^{-3}$, $\epsilon = 3.0/8.1 = 0.37$, and $\kappa = 1.55$), the thermal confinement times deduced for ITER are approximately 5.5 ± 0.9 sec for both the ELMy and ELM-free scalings.

As shown in [4], H-mode confinement in closed divertors is greater than that in open divertors. This was taken into account in developing Eq. 1 by reducing the confinement times in the closed divertor devices (ASDEX and PDX) by a numerical factor, as described in [3] and [5]. In particular, the confinement times for PDX ELMy data were reduced by the factor $(C/R_{D\alpha})^{0.4}$, where $R_{D\alpha}$ is the ratio of D_α emission in the divertor region to that in the midplane, and $C=2$ ($C=3$ was used in [5]). Table 1 shows the effect of varying C within the range of the $R_{D\alpha}$ values in the PDX data (two to six). The top row of values are the coefficients for the ELMy thermal confinement scaling using $C=2$, while the following rows indicate the change in the exponent from the $C=2$ case for the new C . As can be seen from the table, most affected by the change in C are the parametric dependences on R and κ , both weakening with increasing C . The predicted confinement times for ITER (using the EDA parameters) are shown in the last column, and they vary unfavorably from 5.5 sec for $C=2$ to 2.6 sec with $C=6$. These results underscore the importance of describing the divertor action in a quantitatively well determined manner, perhaps by the penetration depth of neutrals into the main chamber.

3. Threshold

The initial analyses of the threshold database [5-7] indicated a nearly linear dependence of threshold power on density, toroidal field, and plasma surface area, S . The threshold database has been extended by including additional data from ASDEX, JET, and high- n_e , high B_T Alcator C-Mod ohmic discharges with a maximum $n_e B_T$ value of $12 \times 10^{20} \text{ m}^{-3} \cdot \text{T}$, extending the range of that value in the original database by a factor of eight, and reaching values in excess of those proposed for ITER. Alcator C-Mod is unique with its Molybdenum first wall. The threshold power in C-Mod was at least a factor of two lower than that suggested by the analysis in [6], and this was achieved without any special wall conditioning. In addition, C-Mod exhibited a weaker dependence of P_{thresh}/S on $n_e B_T$ than did other devices. The threshold database was also augmented by data from boronized conditions on ASDEX-Upgrade, Compass-D, DIII-D, and PBX-M. For the latter two devices, boronization resulted in at least a factor of two reduction in the threshold power over that with non-boronized conditions. A more complete description of the newly added data is found in [7].

In [7], a data subset representing discharges with the lowest threshold powers was selected for analysis. All discharges in this subset were in deuterium, which leads to lower threshold powers than those in hydrogen. Following [7], any power can be expressed in the dimensionally correct form $P \sim nTvS$, where n is density, T is temperature, S is surface area, and v is velocity (which is taken to be the thermal velocity and scale as $\sim(T/M)^{1/2}$), which leads to $P \sim nST^{3/2}M^{-1/2}$. Eliminating $T^{3/2}$ while assuming the expression depends only on dimensionless plasma physics parameters (β , v_* , and ρ_*), and also noting that only deuterium discharges are being compared (M is the same), plausible expressions for the power threshold can be derived [8,9]. These are $P \sim n^{0.75}BS$, where it is assumed that $P \propto BS$, $P \sim nBR^{2.5}$, where it is assumed that $P \propto nB$, and $P \sim nB^{0.6}S$ where it is assumed that $P \propto nS$.

Plots of $\log_{10} P_{\text{tot}}$ as a function of $\log_{10} (n^{0.75}BS)$ and $\log_{10} (nBR^{2.5})$ for the data subset are shown in Figs. 2a and 2b (the third expression results in a similar plot which is not shown here). The straight lines are approximate lower bounds to the threshold power, and are given by the expressions $P_{\text{tot}} = 0.025n_e^{0.75}B_TS$ (Fig. 2a) and $0.4n_eB_TS^{2.5}$ (Fig. 2b) in units of 10^{20} m^{-3} , T , m^2 , m . The scaling with $n_eB_TS^{2.5}$ perhaps exhibits a slightly better ordering of the data near the minimum threshold, except for the Compass-D points which are clearly above the line (the Compass H-modes were achieved by raising density above some threshold value at constant power). In both plots, the C-Mod data fall slightly below the line.

In order to determine the expected power threshold for ITER from these scalings, a target density of $5 \times 10^{19} \text{ m}^{-3}$ is assumed. The first scaling yields a threshold power of $\approx 100 \text{ MW}$, while the second gives $\approx 200 \text{ MW}$. These high values suggest that the transition into the H-mode should be attempted at even lower density, although observations indicate a lower density "threshold" for the H-transition of $2.5 \times 10^{19} \text{ m}^{-3}$; below this value, a substantial increase in heating power is required. Once the H-mode is obtained, however, this phase can be maintained at power levels of order 50% of the threshold power. This hysteresis effect can be exploited by accessing the H-mode at low density, and then increasing density during the H-phase to increase fusion power.

4. L-mode Confinement

The L-mode database [10,11] has been expanded by adding more information about the experimental configuration, conditioning, heating and radiative power, and fast ion population. With 92 variables per time-slice, this update makes the L-mode database more complete and compatible with the H-mode database. The database was extended by both new data from various devices as well as by the addition of data to many pre-existing entries.

At this time, the updated L-mode database consists of 2207 entries from 11 different tokamak devices (ASDEX, DIII, DIII-D, FTU, JET, JFT-2M, JT-60, PBX-M, PDX, TORE-SUPRA, and TEXTOR), consisting of both ohmic (640) and auxiliary heated (1567) time slices, with the largest contributions from JET and JT-60 (325 and 410 auxiliary heated discharges respectively). Most of the auxiliary heated time-slices (1362) are with neutral beams. Of the L-mode discharges, 696 are diverted (583 being single null), and 871 are limited by a material surface. No distinction was made on the basis of auxiliary heating mechanism or limiting surface in the following analysis. There were, however, 84 discharges (62 from TORE-SUPRA) that contained Helium, and these discharges were eliminated for the following analysis.

Figures 3a-c are plots that characterize the parameter range covered by the remaining 1483 L-mode discharges. Some parameter interdependence can be observed in these figures, most notably between plasma current and aspect ratio, and elongation and

toroidal field. Systematic calculations of pairwise correlations indicate that the strongest correlations are between I_p , B_T , total heating power, and plasma size.

Thermal confinement time data is, at present, still being added to the database. Consequently, the database is not yet well enough conditioned to perform any scaling analyses based on the thermal energy confinement time. The results of a power law based multiple linear regression on the eight variables given in Table 2 (excluding $l_z/2$, which has virtually no effect on confinement time in this dataset) gives the following expression for the total (thermal + fast particle) energy confinement time

$$\tau_{\text{tot}} = 0.035 I_p^{0.73} B_T^{0.23} P_L^{-0.57} M^{0.50} R^{1.67} n_e^{0.17} \epsilon^{0.16} \kappa^{0.63} \quad (3)$$

in the same units given for (1) and (2). Here, P_L is defined as ohmic plus auxiliary heating power, less shine-thru for NBI. The root mean square error for the fit is 16.8%, and the experimental values as a function of the fitted values are shown in Fig. 4. In the above expression, the global confinement time from equilibrium magnetics was used except for ASDEX and JT-60 lower X-point divertor discharges, where diamagnetic loop based measurements were used. Equation 3 is distinctly Bohm-like. We caution that Eq. 3 is a preliminary result. The rms error of 16.8% is greater than even the 13.8% rms error of the ELM scaling (Eq. 1). One of the reasons for this is that a careful selection of a standard subset has not yet been done for the L-mode data. In addition, the database has not yet been screened for specific time-slices that may be problematic. These tasks will be performed in the future.

5. Summary and Conclusions

The database activities have led to a more comprehensive set of data from which a better empirical understanding of H-, and L-mode confinement, and H-mode transition requirements has been derived. The studies have defined shortcomings in the present data set, and these indicate areas for future experiments and analysis. Power law scalings of the thermal energy confinement time for both ELM and ELM-free H-modes discharges exhibit a strong size dependence and predict an ITER confinement time of approximately 5.5 sec. The data indicate a major role played by the neutral penetration from the divertor to the main chamber, and how to take this into account affects the predicted ITER confinement time significantly. An approach using dimensionless variables yields expressions for the L- to H-threshold power which predict threshold levels of between 100 and 200 MW for ITER. Finally, the original L-mode database has been extended. Preliminary analysis reproduces the overall parametric dependences seen in scalings based on earlier versions of the L-mode database. Work on deriving the thermal energy confinement scaling and in compiling a profile database for transport model development is in progress.

Acknowledgments

The authors wish to acknowledge Drs. A. Bergmann, H. Maeda and T. Tsunematsu. The work was supported by U.S. Department of Energy Contract No. DE-AC02-76-CHO3073 at PPPL, DE-AC03-89ER51114 at General Atomics, and DE-AC02-78ET51013 at MIT.

References

- [1] CHRISTIANSEN, J.P., et al., Nucl. Fusion 32 (1992) 291-338.
- [2] ITER H-MODE DATABASE WORKING GROUP, Nucl. Fusion 34 (1994) 131-167.

- [3] ITER H-MODE DATABASE WORKING GROUP, in Controlled Fusion and Plasma Physics (Proc. 20th Eur. Conf. Lisbon, 1993) Vol. 17C, Part I, European Physical Society, Geneva (1993) 103-106.
- [4] KAYE, S.M., et al., J.Nucl. Mat. 121 (1984) 115-125.
- [5] ITER H-MODE DATABASE WORKING GROUP, in Plasma Physics and Controlled Nuclear Fusion Research (Proc. 14th Int. Conf. Wurzburg, 1992) Vol. 3, IAEA, Vienna (1993) 251-270.
- [6] ITER H-MODE DATABASE WORKING GROUP, in Controlled Fusion and Plasma Physics (Proc. 20th Eur. Conf. Lisbon, 1993) Vol. 17C, Part I, European Physical Society, Geneva (1993) 15-18.
- [7] ITER H-MODE DATABASE WORKING GROUP, in Controlled Fusion and Plasma Physics (Proc. 21th Eur. Conf. Montpellier, 1994) European Physical Society, Geneva , to be published (1994).
- [8] LACKNER, K., Comments on Plasma Physics and Controlled Fusion 13 (1990) 163-171.
- [9] PERKINS, F., private communication (1993).
- [10] KAYE, S.M. and R.G. GOLDSTON, Nucl. Fusion 25 (1985) 65-69.
- [11] YUSHMANOV, P.G., et al., Nucl. Fusion 30 (1990) 1999-2006.

DISCLAIMER

This report was prepared as an account of work sponsored by an agency of the United States Government. Neither the United States Government nor any agency thereof, nor any of their employees, makes any warranty, express or implied, or assumes any legal liability or responsibility for the accuracy, completeness, or usefulness of any information, apparatus, product, or process disclosed, or represents that its use would not infringe privately owned rights. Reference herein to any specific commercial product, process, or service by trade name, trademark, manufacturer, or otherwise does not necessarily constitute or imply its endorsement, recommendation, or favoring by the United States Government or any agency thereof. The views and opinions of authors expressed herein do not necessarily state or reflect those of the United States Government or any agency thereof.

C	I_P	B_T	P_{Lth}	M	R	n_e	ϵ	κ	τ_E^{ITER}
2	0.76	0.15	-0.70	0.30	2.60	0.42	0.30	1.05	5.6
3	0.13	-0.11	-0.01	0.12	-0.31	-0.06	-0.05	-0.21	5.3
4	0.20	-0.20	-0.01	0.20	-0.51	-0.10	-0.08	-0.37	4.5
5	0.27	-0.27	-0.02	0.26	-0.68	-0.13	-0.10	-0.50	3.7
6	0.32	-0.33	-0.02	0.31	-0.81	-0.16	-0.11	-0.60	2.6

Table 1: Change in ELMy thermal energy confinement time scaling exponent for different re normalization of the PDX confinement times. The ITER confinement prediction (last column) is given in sec.

Figure Captions

Fig. 1 (a) Experimental thermal confinement times vs. scaling value (Eq. 1) for ELM-
H-mode data, (b) Experimental thermal confinement times vs. scaling value (Eq.
2) for ELM-free H-mode data.

Fig. 2 (a) Total power vs. $n_e^{0.75}B_T S$ in log₁₀-log₁₀ representation, (b) Total power vs.
 $n_e B_T R^{2.5}$ in log₁₀-log₁₀ representation.

Fig. 3 Range of parameter values for the L-mode database (a) plasma current vs. aspect
ratio, (b) elongation vs. toroidal field, (c) line averaged density vs. total heating
power

Fig. 4 Experimental global confinement times vs. scaling value (Eq. 3) for L-mode data.

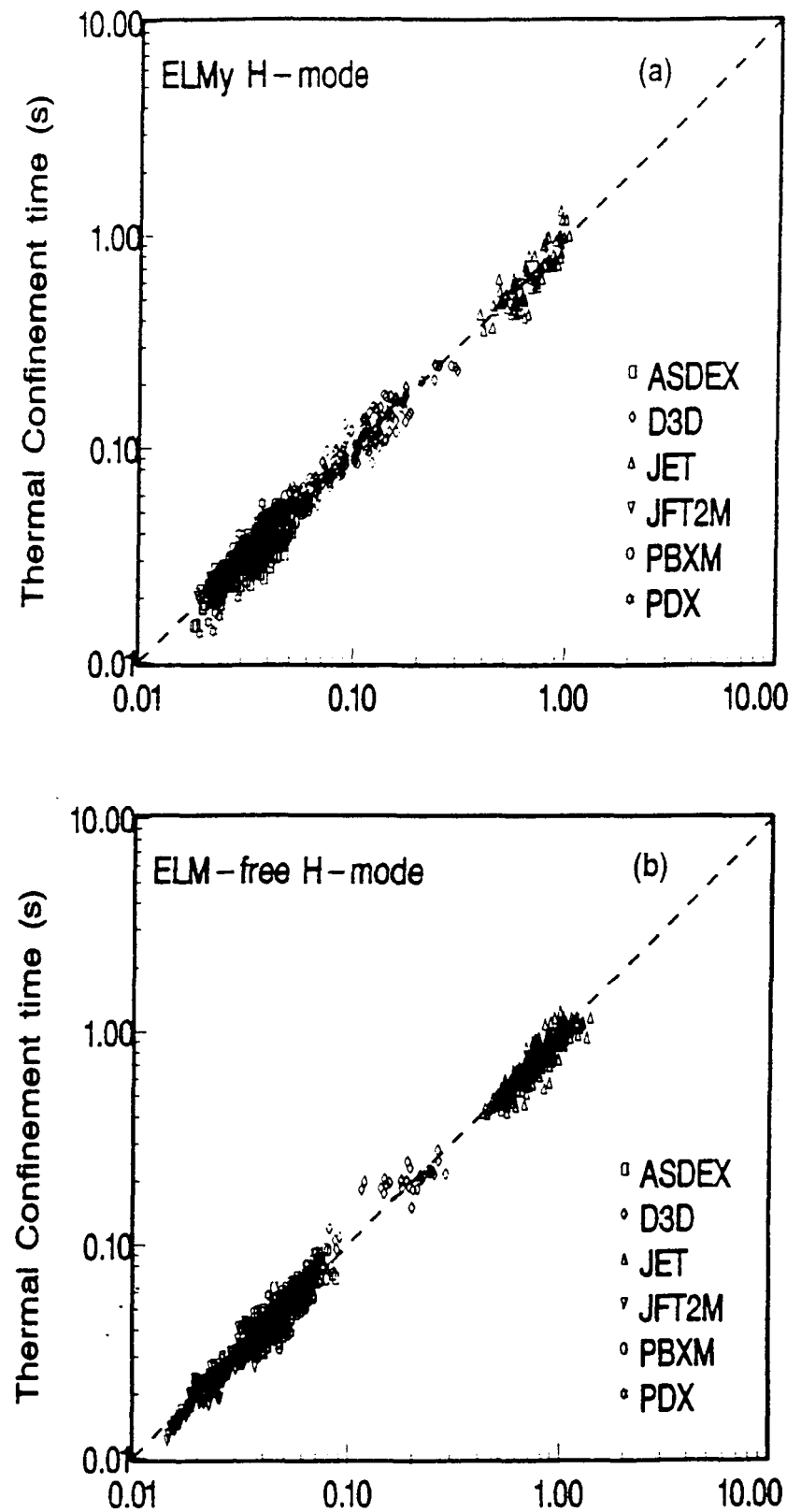


Figure 1

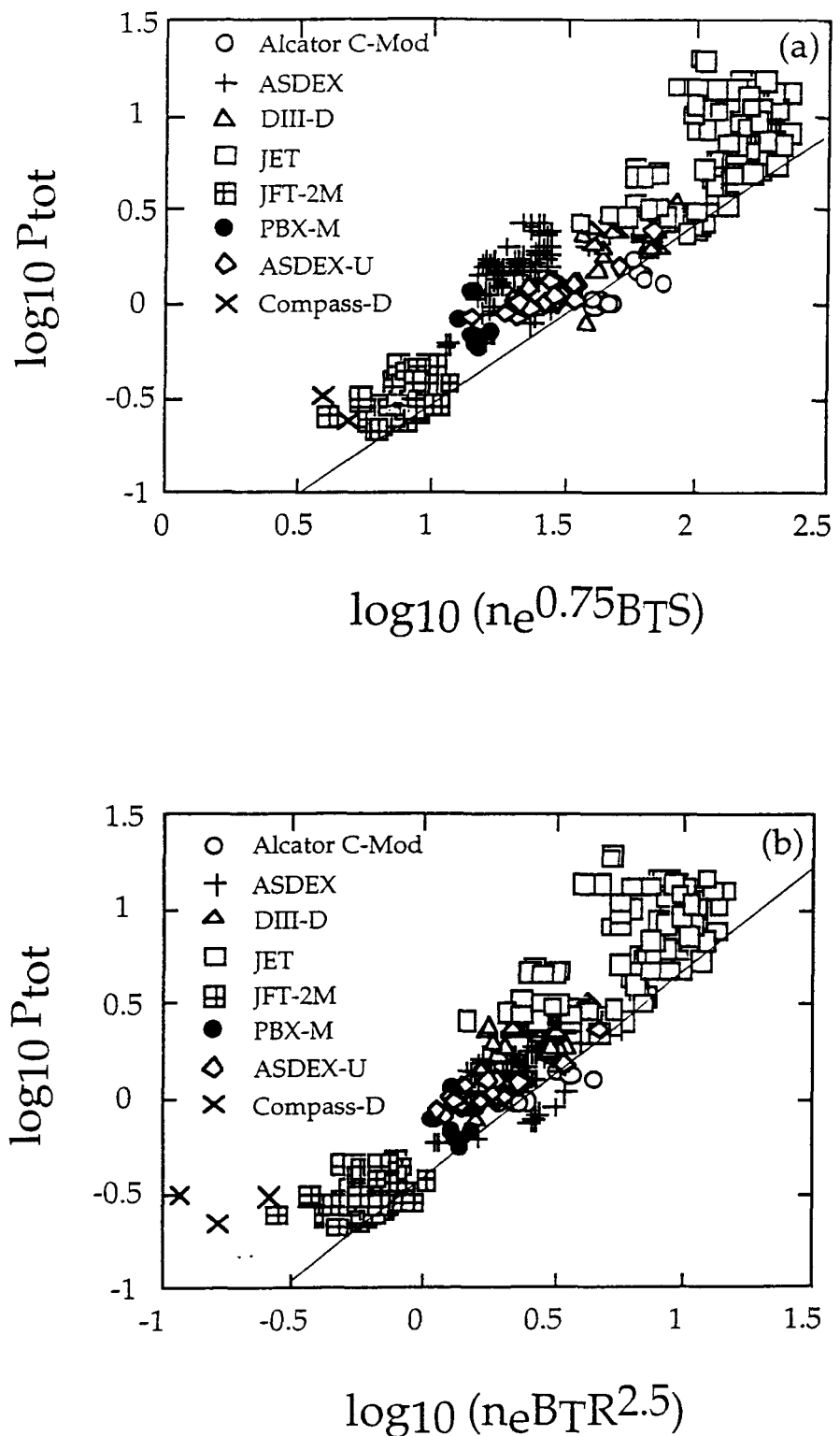


Figure 2

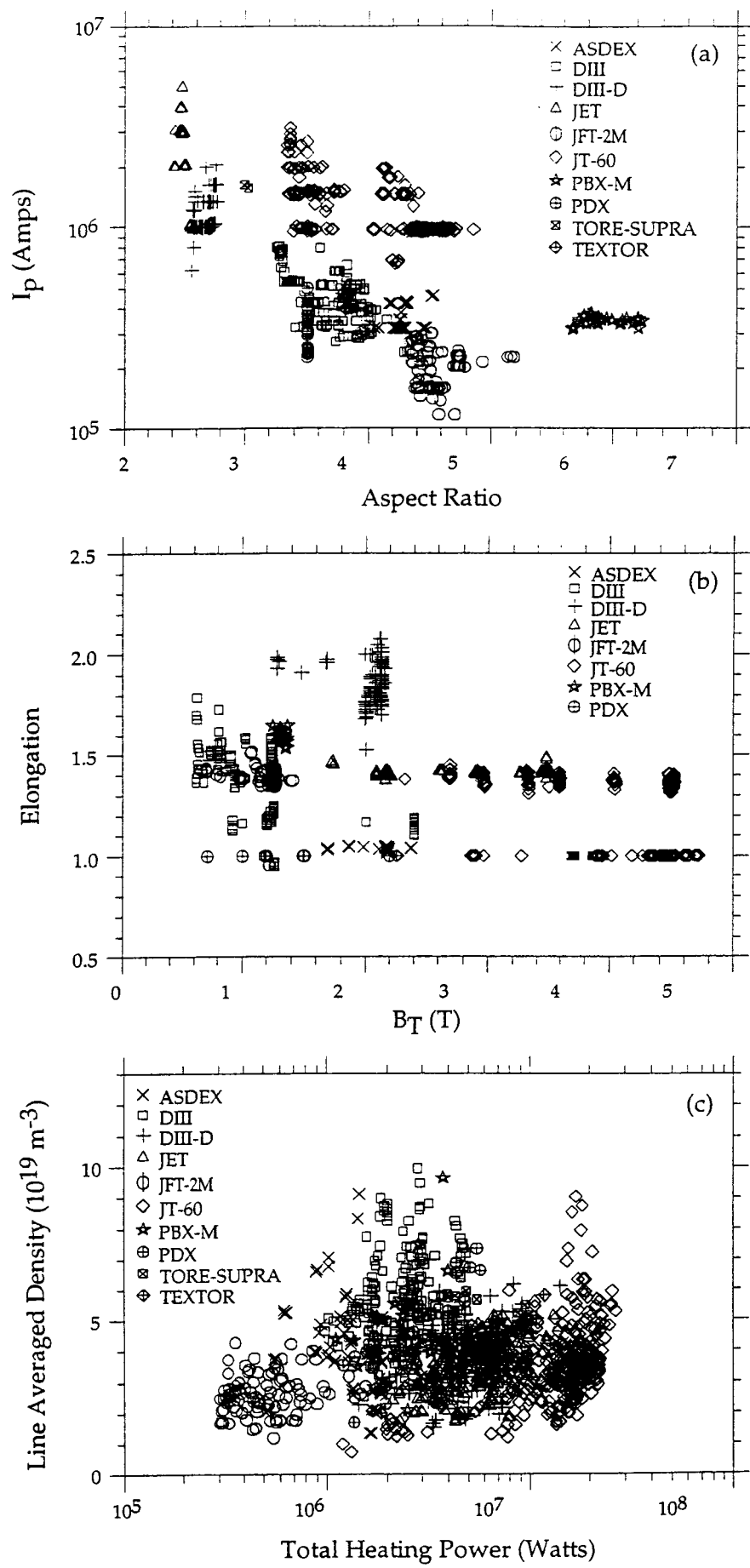


Figure 3

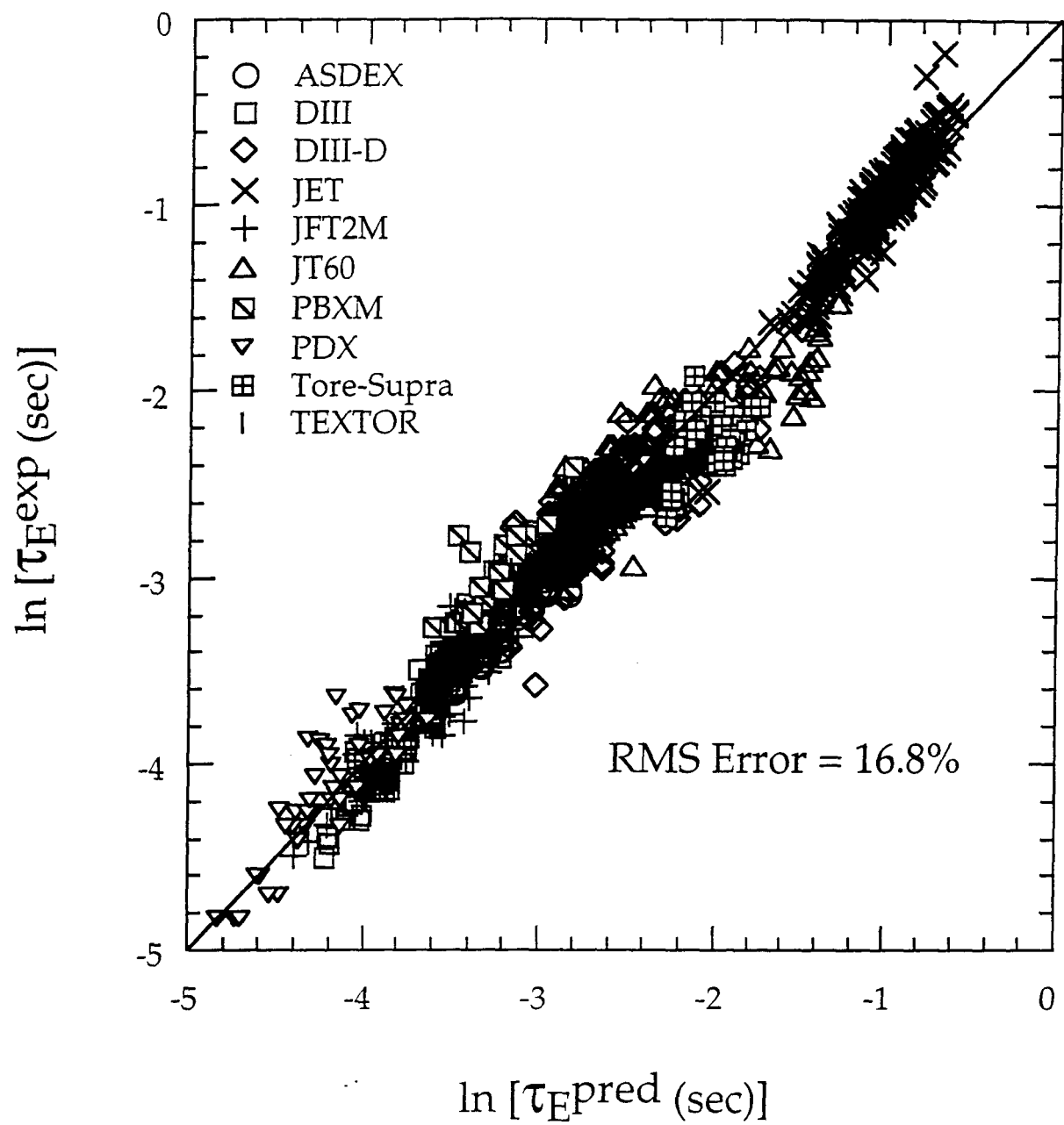


Figure 4